Fermi National Accelerator Laboratory

FERMILAB-Pub-75/69-EXP
7100.007

(Submitted to Phys. Lett. B)

OBSERVATION OF STRUCTURE IN ELASTIC pp SCATTERING AT 100 AND 200 GeV/c

C. W. Akerlof, R. Kotthaus, R. L. Loveless, and D. I. Meyer
Physics Department, University of Michigan, Ann Arbor, Michigan 48104

and

I. Ambats, W. T. Meyer, and C. E. W. Ward
Argonne National Laboratory, Argonne, Illinois 60439

and

D. P. Eartly, R. A. Lundy, S. M. Pruss, and D. D. Yovanovitch
Fermi National Accelerator Laboratory, Batavia, Illinois 60510

and

D. R. Rust
Physics Department, University of Indiana, Bloomington, Indiana 47401

September 1975

Observation of Structure in Elastic PP Scattering at 100 and 200 GeV/c*

C.W. Akerlof, R. Kotthaus,+ R.L. Loveless, D.I. Meyer

Physics Department
University of Michigan
Ann Arbor, Michigan 48104

I. Ambats, W.T. Meyer,† C.E.W. Ward

Argonne National Laboratory
Argonne, Illinois 60439

D.P. Eartly, R.A. Lundy, S.M. Pruss, D.D. Yovanovitch

Fermi National Accelerator Laboratory
Batavia, Illinois 60510

D.R. Rust

Physics Department
University of Indiana
Bloomington, Indiana 47401

Abstract

The elastic differential cross section for pp scattering has been measured up to a momentum transfer of $|t| = 3(\mathrm{GeV/c})^2$ at 100 GeV/c and 200 GeV/c incident momenta. The 200 GeV/c measurement shows a diffractive like dip at $|t| = 1.5$ GeV/c while no such dip is seen in the 100 GeV/c data.

*Work supported by the U.S. E.R.D.A.

+Present address: Max-Planck-Institut fur Physik und Astrophysik, Munchen, W. Germany.

†Present address: Stanford Linear Accelerator Center, Stanford, California.

Several measurements of elastic pp scattering at ISR energies[1,2] in the momentum transfer region, $|t|>1.0$ $(GeV/c)^2$ exhibit a pronounced dip structure in the differential cross section $d\sigma/dt$ at $|t|\approx 1.4$ $(GeV/c)^2$ often attributed to diffractive effects. These measurements span a wide range of center-of-mass energies: 23.5 - 53 GeV corresponding to incident laboratory momenta from 300 GeV/c to 2100 GeV/c. Similar structure has not been observed at laboratory momenta of 33 GeV/c and below, although there is a break in the cross section near this t value.[3]

We have measured pp elastic scattering at 100 and 200 GeV/c incident momentum to examine how this structure develops as a function of energy.

The experiment was performed in the M1E beam of the Meson Area at the Fermi National Accelerator Laboratory. The experimental apparatus shown in Fig. 1 consists of a hydrogen target, a forward spectrometer, and a recoil detector. The forward spectrometer utilized two bending magnets of 20 x 60 cm aperture, each 183 cm long, giving a total $Bd\ell$ of 70 kG meters. Particle track positions were measured with magnetostrictive wire spark chambers arranged in modules of 4 gaps each. Two chambers were aligned to provide (x,y) coordinates and two measured (u,v) coordinates rotated by 30° with respect to the vertical. Three such modules were used in the forward spectrometer; two placed immediately fore and aft of the bending magnets and the third 18.3 meters downstream of the bend center. The momentum resolution of this forward arm was measured to be $\Delta p/p = \pm 1\%$ at 200 GeV/c. The fourth module of spark chambers, containing 6 gaps,

(x,y) and 2 (u,v) type, were used as the recoil detector. Two scintillator hodoscopes of 10 elements in both the horizontal and vertical plane defined the direction of an incident particle. The first hodoscope (not shown in Fig. 1) was 30 m upstream from the hydrogen target. The hodoscopes with a spatial resolution of ±1.5 mm determined incident particle directions to a precision of ±0.07 mrad. The beam was operated with a momentum definition of $\Delta p/p = \pm 0.5\%$ and at an intensity of about 10^6 particles per 0.8 sec long accelerator spill.

The spark chamber trigger required a beam particle, previously labeled by two gas differential Čerenkov counters to be a proton, no signal from a veto counter containing a 2.5 x 2.5 cm hole upstream of the hydrogen counter, and finally signals from scintillators in both the forward and recoil arms. Rather important in rejecting inelastic events was a veto counter (AFI) behind two radiation lengths of Pb 2.5 m downstream of the hydrogen target. A hole in this counter allowed all elastic events to be accepted which were within the magnet aperture while a large fraction of inelastic events were rejected.

The acceptance of this system is mostly determined by the geometry of the recoil arm and is quite uniform for $0.1 \leq |t| \leq 7$ $(\mathrm{GeV/c})^2$. Below a $|t|$ value of 0.1 $(\mathrm{GeV/c})^2$ the short range of the recoil protons and the dimensions of the hydrogen target (4 cm diameter and 30 cm long) reduce the effective acceptance quite rapidly. During some of the data taking the trigger counters F_1 and F_2 were disconnected to suppress triggers with a $|t|$ value ≤ 0.6 $(\mathrm{GeV/c})^2$ which were abundant compared to the total trigger rate with $|t| \geq 0.6$ $(\mathrm{GeV/c})^2$.

The trigger defined above selected approximately equal numbers of elastic and inelastic events at small $|t|$. This ratio became of

the order of one in a hundred at large values of $|t|$. These inelastic events were eliminated by applying appropriate cuts to the momentum of the forward particle, the coplanarity, and the included angle of the forward and recoil particles.

Figure 2 is a scatter plot of events in the opening and coplanarity angles plane. Included in the plot are all events which passed a missing mass cut centered at the proton mass with $\Delta M^2 = \pm 10\ (\mathrm{GeV})^2$ and with a $|t|$ value larger than $0.8\ (\mathrm{GeV/c})^2$. The projections of this scatter plot in both opening angle and coplanarity exhibit elastic peaks with 0.6 mrad (coplanarity) and 0.4 mrad (opening angle) HWHM. These two angular cuts define colinearity in the C.M. frame which corresponds to a momentum imbalance of less than ±75 MeV at 200 GeV/c. The tails on both side of the peaks are taken as inelastic background, assumed to be flat, and subtracted from the signal. The relative amount of this background increases as a function of t and was 10% of the signal at $|t| = 1\ (\mathrm{GeV/c})^2$.

Figure 3 shows the opening angle and coplanarity angle distributions with no background subtraction as a function of t in the dip region for 200 GeV/c incident momentum. The disappearance of the elastic peak from both coplanarity and opening angle distribution in the dip region, $1.35 < |t| < 1.45\ (\mathrm{GeV/c})^2$, and its return at higher $|t|$ values is apparent. This behavior was not observed in the 100 GeV/c data, where the signal remains visible throughout the same range of $|t|$. Therefore, we conclude that the onset of the minimum in the elastic pp scattering occurs somewhere between 100 and 200 GeV/c incident proton momentum.

The $|t|$ resolution in the dip region was $\Delta t = 0.025$ $(GeV/c)^2$ at 200 GeV/c and somewhat better for 100 GeV/c incident momentum. In both cases a limited number of pion events were measured simultaneously - their $|t|$ distribution does not show any similar structure. We can thus rule out spurious effects such as non-uniform spark chamber efficiency, scintillators, etc. as the cause of the observed structure.

The data corrected with a smooth background extrapolation and subtraction under the observed elastic peaks and cut with ±0.5 mr and ±0.8 mr cuts in the opening angle and coplanarity angle is shown in Fig. 4. The overall normalization was obtained from the small angle elastic scattering data taken in the same apparatus during a separate run with F_1, F_2, F_3, and F_4 active.

The accuracy of the small $|t|$ data normalization is ± 7%; however, we have increased the normalization uncertainty to ± 20% to allow for possible variations in system efficiency at high beam rates.

The data also shows indications of a slight bump around $-t = .8$ $(GeV/c)^2$ at both 100 and 200 GeV/c.

The Chou and Yang[4] model successfully predicted the dip in the elastic pp scattering, assuming that the hadronic distribution reflects the charge distribution within the proton. This model, and additional refinements of it[5], predict the dip to occur at $-t \approx 1.4$ $(GeV/c)^2$ using the same parameterization of the E.M. form factors as measured in electron proton scattering. This diffractive like dip is well established at all ISR energies.

Our measurements indicate that the dip develops only above 100 GeV/c incident momentum. There is a parameterization by

Barger and Olsen[6] which predicts the s-dependence of the dip structure. Our data does not contradict that parameterization but is not extensive enough to confirm its major features. A simple interpretation would be that in the absence of a real part in the scattering amplitude, a diffraction dip in the imaginary part is observable at high energies. The filling of the dip structure at lower energies is then due to the real part of the scattering amplitude, which would be expected to be larger at lower energies. The measurements of the ρ parameter, $\rho = \mathrm{Re}\, f\,(s)/\mathrm{Im}\, f\,(s)$ by Bartenev et al[7] show that, at least near 0°, $\rho = 0$ at 200 GeV/c incident momentum.

Acknowledgements

We wish to thank the Fermilab Accelerator staff for the good performance of the accelerator during our runs and to Dr. P. Koehler and the Meson Laboratory staff for assistance in setting up the experiment.

Our special thanks to Dr. R. Thun for valuable comments and assistance in data taking.

References

(1) A. Böhm, M. Bozzo, R. Ellis, H. Foeth, M.I. Ferrero, G. Maderni, B. Naroska, C. Rubbia, G. Sette, A. Staude, P. Strolin, and G. DeZorzi, Phys. Letters, 49B, (1974) 491.

(2) E. Nagy et al., see: A.N. Diddens: XVII Rochester Conf. Report.

(3) J.V. Allaby et al., Nucl. Phys, B52 (1973) 316.

(4) T. T. Wu and C. N. Yang, Phys. Rev. 137B (1965) B708; T. T. Chou and C. N. Yang, Phys. Rev. 170 (1968) 1591; and Phys. Rev. Letters 20 (1968) 1213.

(5) L. Durand and R. Lipes, Phys. Rev. Letters 20 (1968) 637; and M. Elitzur and R.G. Lipes, Phys. Rev. D7 (1973) 1420.

(6) R.J.N. Phillips and V. Barger, Phys. Letters 46B (1973) 412.

(7) V. Bartenev et al., Phys. Rev. Letters 31 (1973) 1367.

Figure Captions

Figure 1. The experimental set-up. Note 10:1 foreshortening along the incident beam direction.

Figure 2. Scatter plot of events in opening angle-coplanarity plane. Included are the events with $|t|>0.8$ $(\mathrm{GeV}/c)^2$. The projected distribution in either opening angle or coplanarity are also shown.

Figure 3. Opening angle and coplanarity distributions as a function of momentum transfer $|t|$.

Figure 4. Differential cross sections $d\sigma/dt$ for 100 and 200 GeV/c incident momenta.

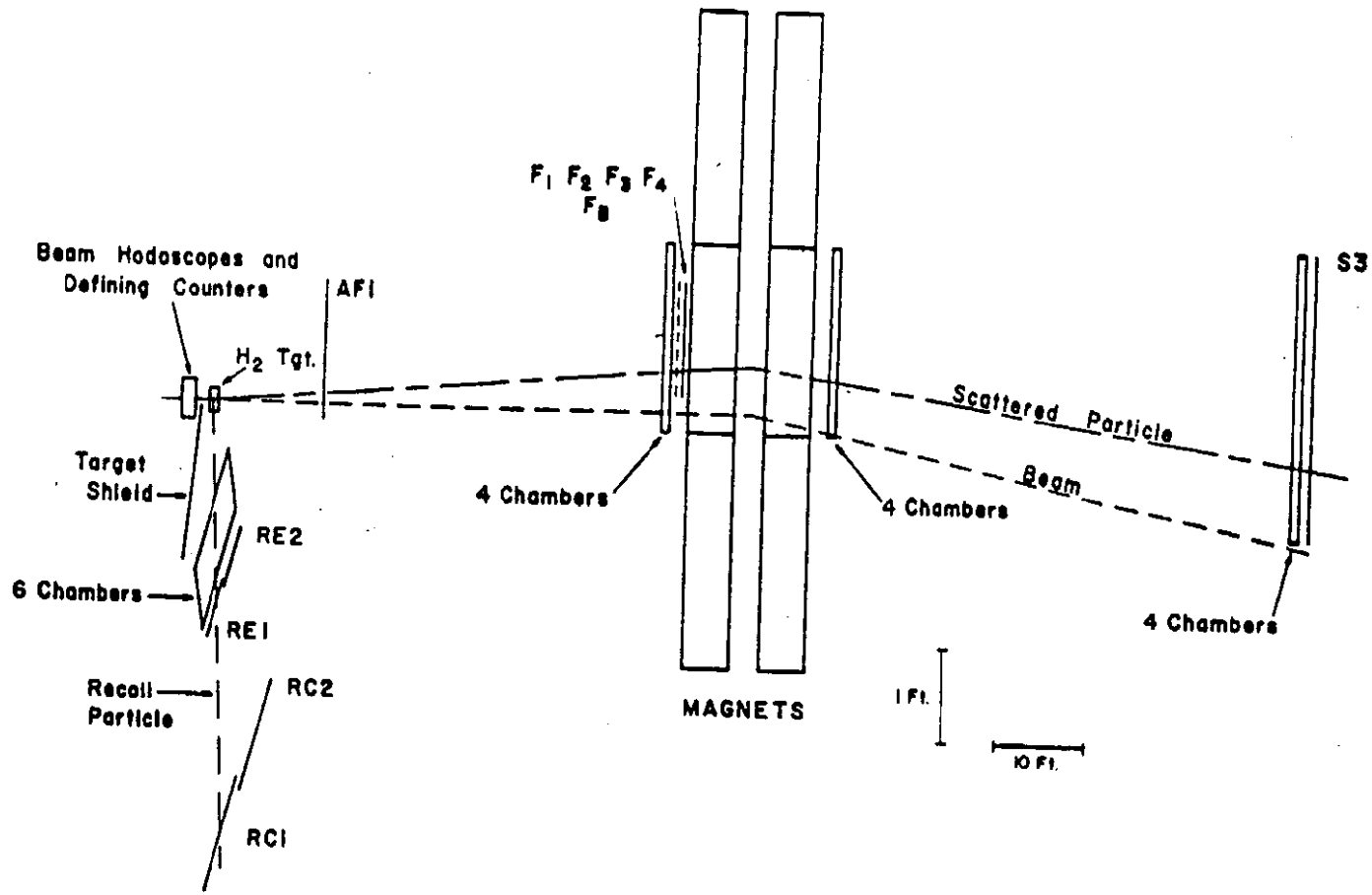
Beam Hodoscopes and
Defining Counters
AF1
H_2 Tgt.
Target
Shield
RE2
6 Chambers
RE1
Recoil
Particle
RC2
RC1
F_1 F_2 F_3 F_4
F_B
4 Chambers
MAGNETS
4 Chambers
Scattered Particle
Beam
S3
4 Chambers
1 Ft.
10 Ft.

Fig. 1

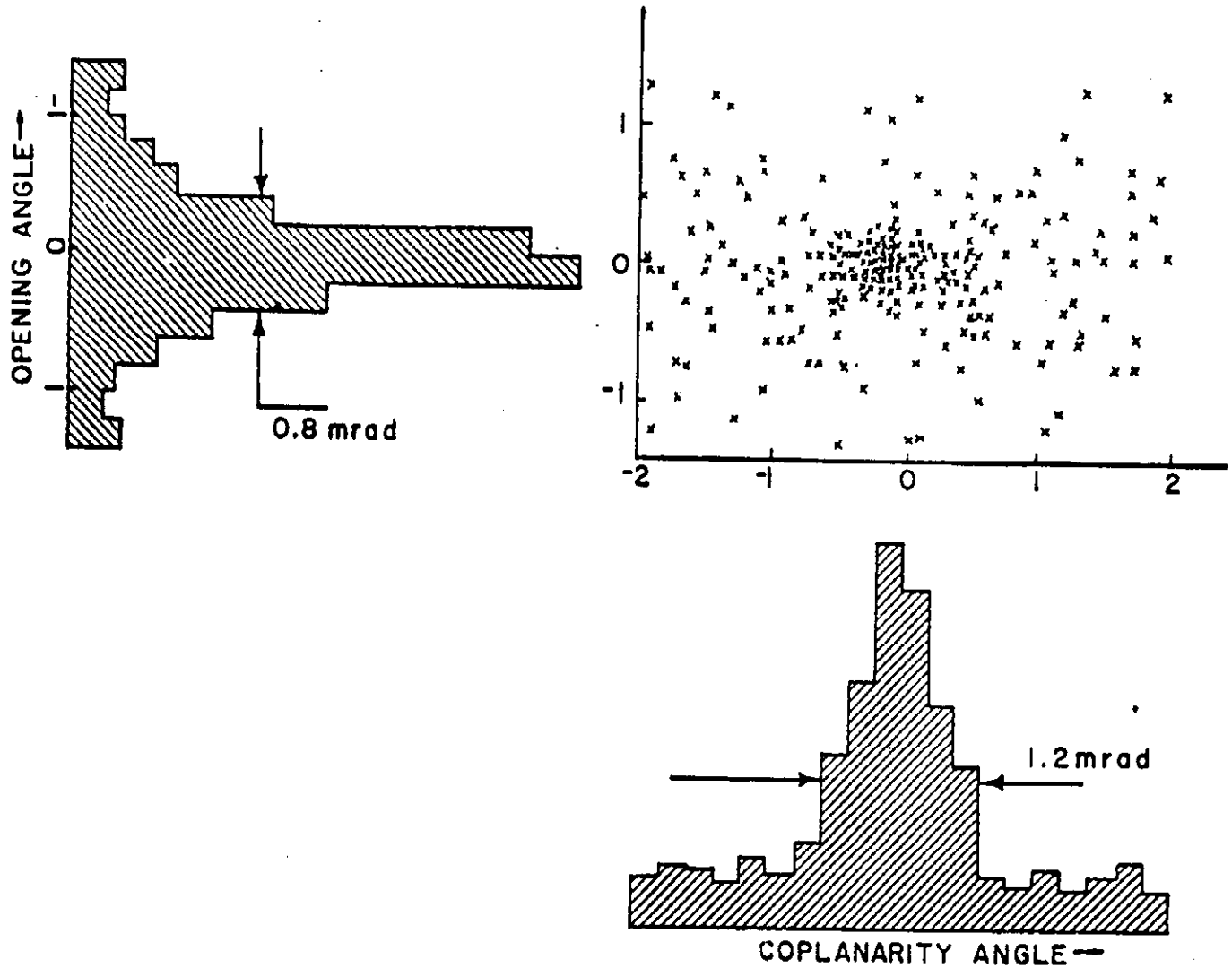
OPENING ANGLE
1
0
-1
0.8 mrad
1
0
-1
-2
-1
0
1
2
1.2 mrad
COPLANARITY ANGLE

Fig. 2

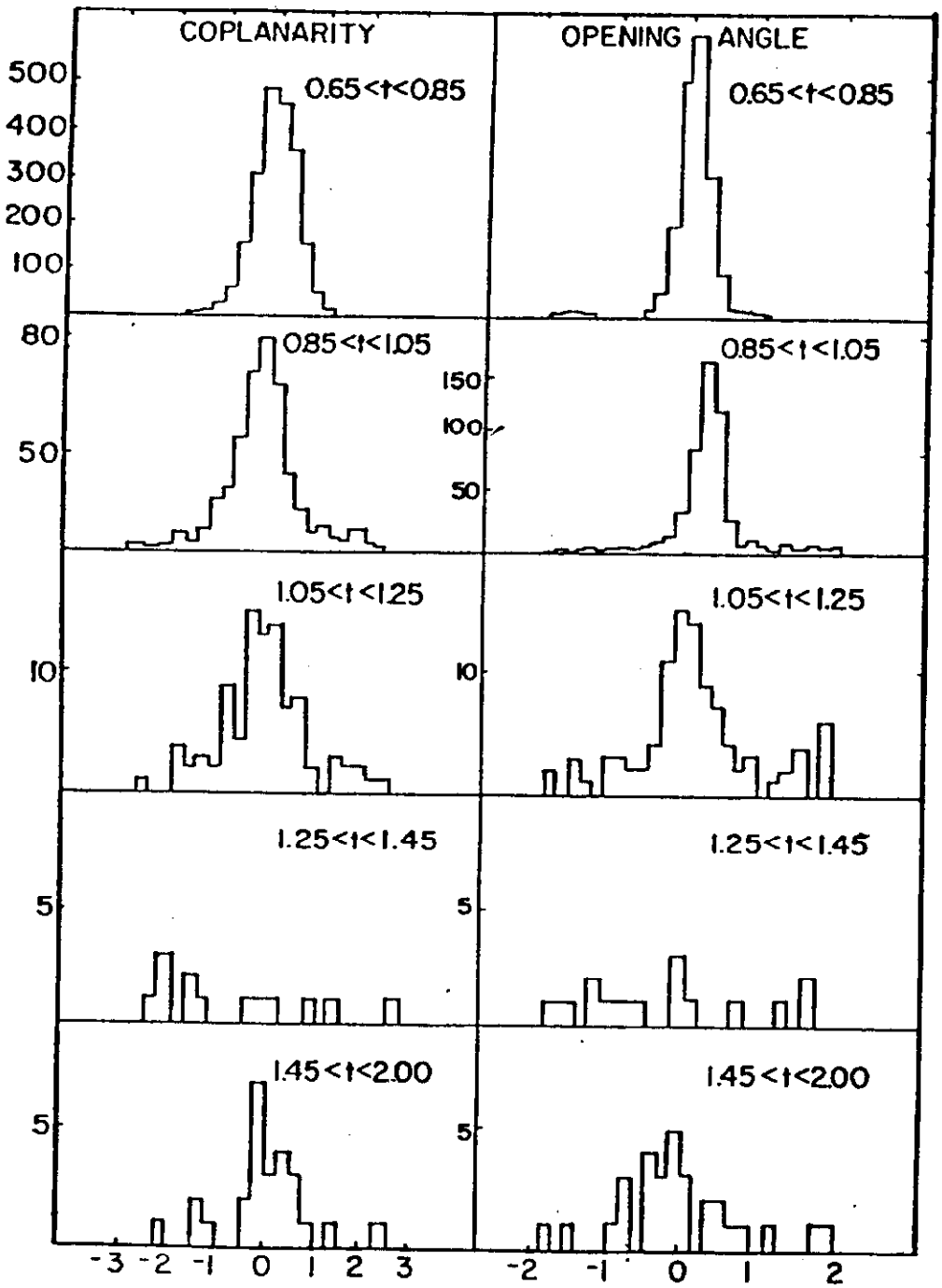
COPLANARITY
OPENING ANGLE
0.65<t<0.85
0.85<t<1.05
1.05<t<1.25
1.25<t<1.45
1.45<t<2.00
500
400
300
200
100
80
50
150
100
50
10
5
-3 -2 -1 0 1 2 3
-2 -1 0 1 2

Fig. 3

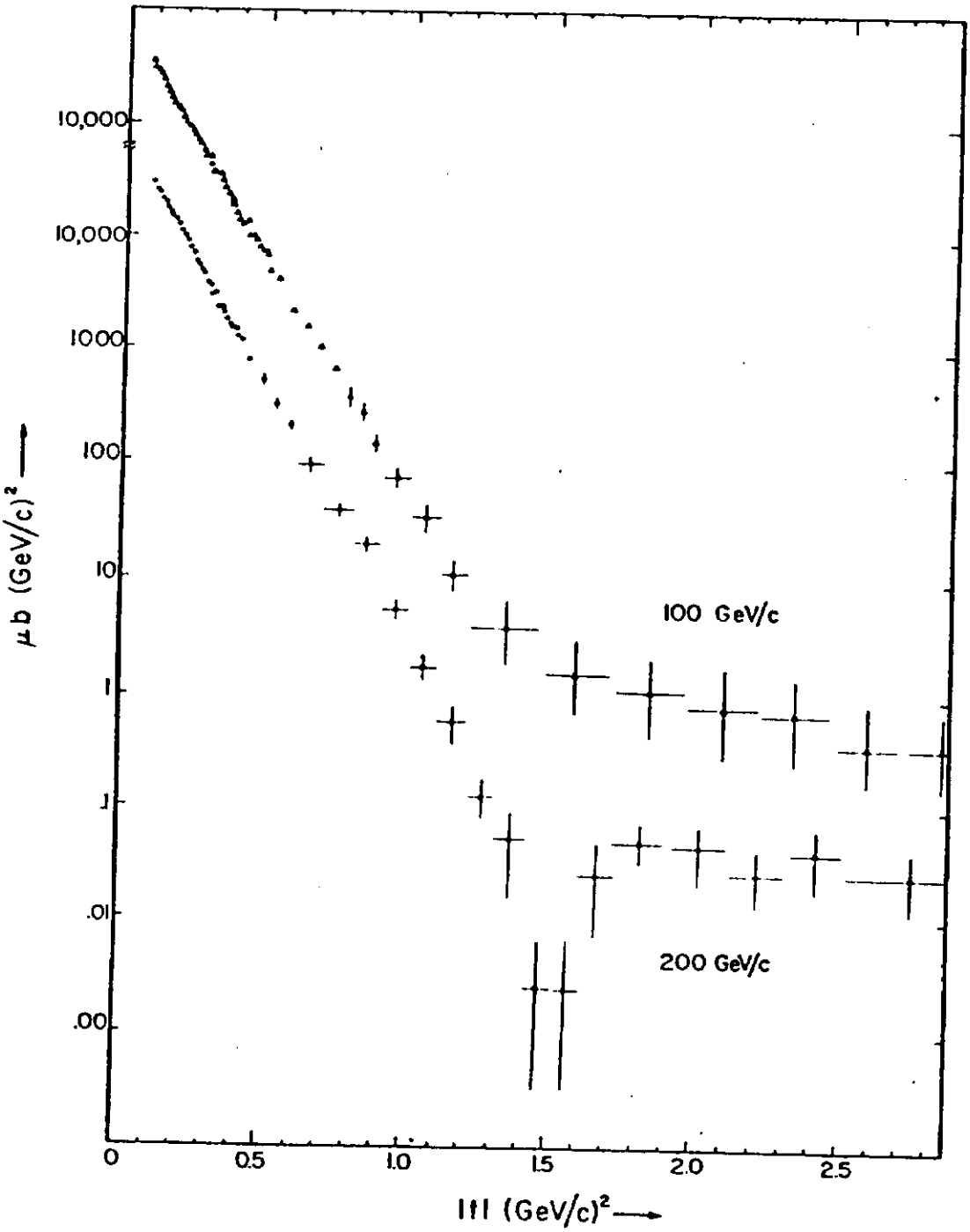
10,000
10,000
1000
100
10
1
.1
.01
.00
μb (GeV/c)²
100 GeV/c
200 GeV/c
0
0.5
1.0
1.5
2.0
2.5
|t| (GeV/c)²

Fig. 4